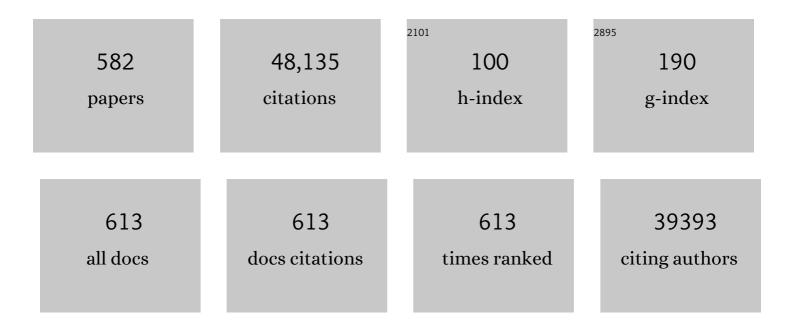
Daniel Rueckert

List of Publications by Year in descending order

Source: https://exaly.com/author-pdf/5116447/publications.pdf Version: 2024-02-01



#	Article	IF	CITATIONS
1	Prediction of complications and surgery duration in primary TKA with high accuracy using machine learning with arthroplasty-specific data. Knee Surgery, Sports Traumatology, Arthroscopy, 2023, 31, 1323-1333.	4.2	20
2	Developing and validating a multivariable prediction model which predicts progression of intermediate to late age-related macular degeneration—the PINNACLE trial protocol. Eye, 2023, 37, 1275-1283.	2.1	9
3	Learning a Model-Driven Variational Network for Deformable Image Registration. IEEE Transactions on Medical Imaging, 2022, 41, 199-212.	8.9	9
4	Exploring a new paradigm for the fetal anomaly ultrasound scan: Artificial intelligence in real time. Prenatal Diagnosis, 2022, 42, 49-59.	2.3	16
5	Zen and the art of model adaptation: Low-utility-cost attack mitigations in collaborative machine learning. Proceedings on Privacy Enhancing Technologies, 2022, 2022, 274-290.	2.8	4
6	Neurocognitive correlates of probable posttraumatic stress disorder following traumatic brain injury. Brain and Spine, 2022, 2, 100854.	0.1	5
7	Video Summarization Through Reinforcement Learning With a 3D Spatio-Temporal U-Net. IEEE Transactions on Image Processing, 2022, 31, 1573-1586.	9.8	40
8	Machine learning in knee arthroplasty: specific data are key—a systematic review. Knee Surgery, Sports Traumatology, Arthroscopy, 2022, 30, 376-388.	4.2	30
9	sPLINK: a hybrid federated tool as a robust alternative to meta-analysis in genome-wide association studies. Genome Biology, 2022, 23, 32.	8.8	18
10	Effect of frailty on 6-month outcome after traumatic brain injury: a multicentre cohort study with external validation. Lancet Neurology, The, 2022, 21, 153-162.	10.2	34
11	Self-Supervised Learning for Few-Shot Medical Image Segmentation. IEEE Transactions on Medical Imaging, 2022, 41, 1837-1848.	8.9	35
12	Al-Based Reconstruction for Fast MRI—A Systematic Review and Meta-Analysis. Proceedings of the IEEE, 2022, 110, 224-245.	21.3	57
13	Artificial Intelligence in Medicine and Privacy Preservation. , 2022, , 145-158.		0
14	Precision measurement of cardiac structure and function in cardiovascular magnetic resonance using machine learning. Journal of Cardiovascular Magnetic Resonance, 2022, 24, 16.	3.3	30
15	Concept of the Munich/Augsburg Consortium Precision in Mental Health for the German Center of Mental Health. Frontiers in Psychiatry, 2022, 13, 815718.	2.6	2
16	Neonatal multi-modal cortical profiles predict 18-month developmental outcomes. Developmental Cognitive Neuroscience, 2022, 54, 101103.	4.0	11
17	Extended Coagulation Profiling in Isolated Traumatic Brain Injury: A CENTER-TBI Analysis. Neurocritical Care, 2022, 36, 927-941.	2.4	4
18	Effects of gestational age at birth on perinatal structural brain development in healthy termâ€born babies. Human Brain Mapping, 2022, 43, 1577-1589.	3.6	3

ARTICLE IF CITATIONS Prediction of Complications and Surgery Duration in Primary Total Hip Arthroplasty Using Machine Learning: The Necessity of Modified Algorithms and Specific Data. Journal of Clinical Medicine, 2022, 11, 2.4 2147. Genetic and environmental determinants of diastolic heart function., 2022, 1, 361-371. 20 12 Multi-Modal Unsupervised Brain Image Registration Using Edge Maps., 2022, , . Harnessing feature extraction capacities from a pre-trained convolutional neural network (VGC-16) for the unsupervised distinction of aortic outflow velocity profiles in patients with severe aortic 22 1.7 6 stenosis. European Heart Journal Digital Health, 2022, 3, 153-168. Surgery versus conservative treatment for traumatic acute subdural haematoma: a prospective, 10.2 26 multicentre, observational, comparative effectiveness study. Lancet Neurology, The, 2022, 21, 620-631. Serum metabolome associated with severity of acute traumatic brain injury. Nature Communications, 24 12.8 29 2022, 13, 2545. Predicting age and clinical risk from the neonatal connectome. NeuroImage, 2022, 257, 119319. 4.2 Privacy: An Axiomatic Approach. Entropy, 2022, 24, 714. 2.2 26 3 The Developing Human Connectome Project Neonatal Data Release. Frontiers in Neuroscience, 2022, 16, 2.8 Health care utilization and outcomes in older adults after Traumatic Brain Injury: A CENTER-TBI study. 28 1.7 11 Injury, 2022, 53, 2774-2782. The developing brain structural and functional connectome fingerprint. Developmental Cognitive 4.0 Neuroscience, 2022, 55, 101117. Cardiac segmentation on late gadolinium enhancement MRI: A benchmark study from multi-sequence 30 11.6 22 cardiac MR segmentation challenge. Medical Image Analysis, 2022, 81, 102528. Prediction of Global Functional Outcome and Post-Concussive Symptoms after Mild Traumatic Brain Injury: External Validation of Prognostic Models in the Collaborative European NeuroTrauma 3.4 Effectiveness Research in Traumatic Brain Injury (CENTER-TBI) Study. Journal of Neurotrauma, 2021, 38, 196-209. Differences between Men and Women in Treatment and Outcome after Traumatic Brain Injury. Journal 32 3.4 39 of Neurotrauma, 2021, 38, 235-251. Late-Gadolinium Enhancement Interface Area and Electrophysiological Simulations Predict Arrhythmic Events in Patients With Nonischemic Dilated Cardiomyopathy. JACC: Clinical 3.2 Electrophysiology, 2021, 7, 238-249. Frequency of fatigue and its changes in the first 6Âmonths after traumatic brain injury: results from 34 3.6 12 the CENTÉR-TBI study. Journal of Neurology, 2021, 268, 61-73. A global benchmark of algorithms for segmenting the left atrium from late gadolinium-enhanced 11.6 150 cardiac magnetic resonance imaging. Medical Image Analysis, 2021, 67, 101832. Automated analysis and detection of abnormalities in transaxial anatomical cardiovascular magnetic resonance images: a proof of concept study with potential to optimize image acquisition. 36 1.5 6

DANIEL RUECKERT

36 resonance images: a proof of concept study with potential to optimize image acquisition. International Journal of Cardiovascular Imaging, 2021, 37, 1033-1042.

#	Article	IF	CITATIONS
37	Global Characterisation of Coagulopathy in Isolated Traumatic Brain Injury (iTBI): A CENTER-TBI Analysis. Neurocritical Care, 2021, 35, 184-196.	2.4	21
38	<scp>T1</scp> , <scp>T2,</scp> and Fat Fraction Cardiac MR Fingerprinting: Preliminary Clinical Evaluation. Journal of Magnetic Resonance Imaging, 2021, 53, 1253-1265.	3.4	27
39	CAS-Net: Conditional Atlas Generation and Brain Segmentation for Fetal MRI. Lecture Notes in Computer Science, 2021, , 221-230.	1.3	2
40	Evaluation of the Robustness of Learned MR Image Reconstruction to Systematic Deviations Between Training and Test Data for the Models from the fastMRI Challenge. Lecture Notes in Computer Science, 2021, , 25-34.	1.3	3
41	Multiscale Graph Convolutional Networks for Cardiac Motion Analysis. Lecture Notes in Computer Science, 2021, , 264-272.	1.3	5
42	Artificial Intelligence in Medicine and Privacy Preservation. , 2021, , 1-14.		1
43	Cooperative Training and Latent Space Data Augmentation for Robust Medical Image Segmentation. Lecture Notes in Computer Science, 2021, , 149-159.	1.3	12
44	Joint Motion Correction and Super Resolution for Cardiac Segmentation viaÂLatent Optimisation. Lecture Notes in Computer Science, 2021, , 14-24.	1.3	9
45	Mutual Information-Based Disentangled Neural Networks for Classifying Unseen Categories in Different Domains: Application to Fetal Ultrasound Imaging. IEEE Transactions on Medical Imaging, 2021, 40, 722-734.	8.9	28
46	Federated deep learning for detecting COVID-19 lung abnormalities in CT: a privacy-preserving multinational validation study. Npj Digital Medicine, 2021, 4, 60.	10.9	134
47	The Developing Human Connectome Project: typical and disrupted perinatal functional connectivity. Brain, 2021, 144, 2199-2213.	7.6	75
48	Phenotyping the Preterm Brain: Characterizing Individual Deviations From Normative Volumetric Development in Two Large Infant Cohorts. Cerebral Cortex, 2021, 31, 3665-3677.	2.9	19
49	De Novo Radiomics Approach Using Image Augmentation and Features From T1 Mapping to Predict Gleason Scores in Prostate Cancer. Investigative Radiology, 2021, 56, 661-668.	6.2	18
50	Dynamic Spatio-Temporal Graph Convolutional Networks For Cardiac Motion Analysis. , 2021, , .		7
51	End-to-end privacy preserving deep learning on multi-institutional medical imaging. Nature Machine Intelligence, 2021, 3, 473-484.	16.0	157
52	A Review of Deep Learning in Medical Imaging: Imaging Traits, Technology Trends, Case Studies With Progress Highlights, and Future Promises. Proceedings of the IEEE, 2021, 109, 820-838.	21.3	339
53	Systematic evaluation of iterative deep neural networks for fast parallel MRI reconstruction with sensitivityâ€weighted coil combination. Magnetic Resonance in Medicine, 2021, 86, 1859-1872.	3.0	39
54	Medical imaging deep learning with differential privacy. Scientific Reports, 2021, 11, 13524.	3.3	52

#	Article	IF	CITATIONS
55	Missing Data in Prediction Research: A Five-Step Approach for Multiple Imputation, Illustrated in the CENTER-TBI Study. Journal of Neurotrauma, 2021, 38, 1842-1857.	3.4	16
56	Complementary timeâ€frequency domain networks for dynamic parallel MR image reconstruction. Magnetic Resonance in Medicine, 2021, 86, 3274-3291.	3.0	21
57	Incidental findings on brain MR imaging of asymptomatic term neonates in the Developing Human Connectome Project. EClinicalMedicine, 2021, 38, 100984.	7.1	16
58	Efficient, high-performance semantic segmentation using multi-scale feature extraction. PLoS ONE, 2021, 16, e0255397.	2.5	9
59	Occurrence and timing of withdrawal of life-sustaining measures in traumatic brain injury patients: a CENTER-TBI study. Intensive Care Medicine, 2021, 47, 1115-1129.	8.2	31
60	Primary versus early secondary referral to a specialized neurotrauma center in patients with moderate/severe traumatic brain injury: a CENTER TBI study. Scandinavian Journal of Trauma, Resuscitation and Emergency Medicine, 2021, 29, 113.	2.6	8
61	Pathological Computed Tomography Features Associated With Adverse Outcomes After Mild Traumatic Brain Injury. JAMA Neurology, 2021, 78, 1137.	9.0	53
62	Phenotypic Expression and Outcomes in Individuals With Rare Genetic Variants of Hypertrophic Cardiomyopathy. Journal of the American College of Cardiology, 2021, 78, 1097-1110.	2.8	55
63	Al for Doctors—A Course to Educate Medical Professionals in Artificial Intelligence for Medical Imaging. Healthcare (Switzerland), 2021, 9, 1278.	2.0	16
64	Adversarial interference and its mitigations in privacy-preserving collaborative machine learning. Nature Machine Intelligence, 2021, 3, 749-758.	16.0	26
65	Preterm birth alters the development of cortical microstructure and morphology at term-equivalent age. NeuroImage, 2021, 243, 118488.	4.2	40
66	Transductive Image Segmentation: Self-training and Effect of Uncertainty Estimation. Lecture Notes in Computer Science, 2021, , 79-89.	1.3	0
67	Detecting Hypo-plastic Left Heart Syndrome in Fetal Ultrasound via Disease-Specific Atlas Maps. Lecture Notes in Computer Science, 2021, , 207-217.	1.3	8
68	Improving Phenotype Prediction Using Long-Range Spatio-Temporal Dynamics of Functional Connectivity. Lecture Notes in Computer Science, 2021, , 145-154.	1.3	3
69	Deep Learningâ€Based Automated Abdominal Organ Segmentation in the UK Biobank and German National Cohort Magnetic Resonance Imaging Studies. Investigative Radiology, 2021, 56, 401-408.	6.2	30
70	Reducing Textural Bias Improves Robustness of Deep Segmentation Models. Lecture Notes in Computer Science, 2021, , 294-304.	1.3	1
71	Explaining Outcome Differences between Men and Women following Mild Traumatic Brain Injury. Journal of Neurotrauma, 2021, 38, 3315-3331.	3.4	34
72	Questionnaires vs Interviews for the Assessment of Global Functional Outcomes After Traumatic Brain Injury. JAMA Network Open, 2021, 4, e2134121.	5.9	5

#	Article	IF	CITATIONS
73	Flimma: a federated and privacy-aware tool for differential gene expression analysis. Genome Biology, 2021, 22, 338.	8.8	10
74	Motion-Guided Physics-Based Learning for Cardiac MRI Reconstruction. , 2021, , .		8
75	Can We Cluster ICU Treatment Strategies for Traumatic Brain Injury by Hospital Treatment Preferences?. Neurocritical Care, 2021, , 1.	2.4	3
76	Global Burden of Small Vessel Disease–Related Brain Changes on MRI Predicts Cognitive and Functional Decline. Stroke, 2020, 51, 170-178.	2.0	115
77	Model-Based and Data-Driven Strategies in Medical Image Computing. Proceedings of the IEEE, 2020, 108, 110-124.	21.3	30
78	Explainable Anatomical Shape Analysis Through Deep Hierarchical Generative Models. IEEE Transactions on Medical Imaging, 2020, 39, 2088-2099.	8.9	34
79	Water–fat Dixon cardiac magnetic resonance fingerprinting. Magnetic Resonance in Medicine, 2020, 83, 2107-2123.	3.0	48
80	Prognostic Validation of the NINDS Common Data Elements for the Radiologic Reporting of Acute Traumatic Brain Injuries: A CENTER-TBI Study. Journal of Neurotrauma, 2020, 37, 1269-1282.	3.4	10
81	Limited One-time Sampling Irregularity Map (LOTS-IM) for Automatic Unsupervised Assessment of White Matter Hyperintensities and Multiple Sclerosis Lesions in Structural Brain Magnetic Resonance Images. Computerized Medical Imaging and Graphics, 2020, 79, 101685.	5.8	12
82	Reduced structural connectivity in cortico-striatal-thalamic network in neonates with congenital heart disease. NeuroImage: Clinical, 2020, 28, 102423.	2.7	14
83	The developing Human Connectome Project (dHCP) automated resting-state functional processing framework for newborn infants. NeuroImage, 2020, 223, 117303.	4.2	81
84	Predictors of Access to Rehabilitation in the Year Following Traumatic Brain Injury: A European Prospective and Multicenter Study. Neurorehabilitation and Neural Repair, 2020, 34, 814-830.	2.9	12
85	Tracheal intubation in traumatic brain injury: a multicentre prospective observational study. British Journal of Anaesthesia, 2020, 125, 505-517.	3.4	19
86	CINENet: deep learning-based 3D cardiac CINE MRI reconstruction with multi-coil complex-valued 4D spatio-temporal convolutions. Scientific Reports, 2020, 10, 13710.	3.3	122
87	Discriminating electrocardiographic responses to His-bundle pacing using machine learning. Cardiovascular Digital Health Journal, 2020, 1, 11-20.	1.3	10
88	Volume Change in Frontal Cholinergic Structures After Traumatic Brain Injury and Cognitive Outcome. Frontiers in Neurology, 2020, 11, 832.	2.4	5
89	A population-based phenome-wide association study of cardiac and aortic structure and function. Nature Medicine, 2020, 26, 1654-1662.	30.7	98
90	A dataâ€driven approach to optimising the encoding for multiâ€shell diffusion MRI with application to neonatal imaging. NMR in Biomedicine, 2020, 33, e4348.	2.8	18

#	Article	IF	CITATIONS
91	Investigating altered brain development in infants with congenital heart disease using tensor-based morphometry. Scientific Reports, 2020, 10, 14909.	3.3	17
92	Genetic and functional insights into the fractal structure of the heart. Nature, 2020, 584, 589-594.	27.8	86
93	Multiclass semantic segmentation and quantification of traumatic brain injury lesions on head CT using deep learning: an algorithm development and multicentre validation study. The Lancet Digital Health, 2020, 2, e314-e322.	12.3	83
94	Impact of Antithrombotic Agents on Radiological Lesion Progression in Acute Traumatic Brain Injury: A CENTER-TBI Propensity-Matched Cohort Analysis. Journal of Neurotrauma, 2020, 37, 2069-2080.	3.4	22
95	Parental age effects on neonatal white matter development. NeuroImage: Clinical, 2020, 27, 102283.	2.7	12
96	Development of Microstructural and Morphological Cortical Profiles in the Neonatal Brain. Cerebral Cortex, 2020, 30, 5767-5779.	2.9	42
97	Secure, privacy-preserving and federated machine learning in medical imaging. Nature Machine Intelligence, 2020, 2, 305-311.	16.0	473
98	Deep Learning for Cardiac Image Segmentation: A Review. Frontiers in Cardiovascular Medicine, 2020, 7, 25.	2.4	467
99	Improving ultrasound video classification: an evaluation of novel deep learning methods in echocardiography. Journal of Medical Artificial Intelligence, 2020, 3, 4-4.	1.1	31
100	Sparse Data–Driven Learning for Effective and Efficient Biomedical Image Segmentation. Annual Review of Biomedical Engineering, 2020, 22, 127-153.	12.3	3
101	Improving the Generalizability of Convolutional Neural Network-Based Segmentation on CMR Images. Frontiers in Cardiovascular Medicine, 2020, 7, 105.	2.4	74
102	Large-scale Quality Control of Cardiac Imaging in Population Studies: Application to UK Biobank. Scientific Reports, 2020, 10, 2408.	3.3	22
103	Heterogeneity in Brain Microstructural Development Following Preterm Birth. Cerebral Cortex, 2020, 30, 4800-4810.	2.9	54
104	Evaluating severity of white matter lesions from computed tomography images with convolutional neural network. Neuroradiology, 2020, 62, 1257-1263.	2.2	8
105	Deep Learning for Cardiac Motion Estimation: Supervised vs. Unsupervised Training. Lecture Notes in Computer Science, 2020, , 186-194.	1.3	6
106	Going Deeper into Cardiac Motion Analysis to Model Fine Spatio-Temporal Features. Communications in Computer and Information Science, 2020, , 294-306.	0.5	5
107	Self-supervision with Superpixels: Training Few-Shot Medical Image Segmentation Without Annotation. Lecture Notes in Computer Science, 2020, , 762-780.	1.3	83
108	Realistic Adversarial Data Augmentation for MR Image Segmentation. Lecture Notes in Computer Science, 2020, , 667-677.	1.3	32

#	Article	IF	CITATIONS
109	Biomechanics-Informed Neural Networks for Myocardial Motion Tracking in MRI. Lecture Notes in Computer Science, 2020, , 296-306.	1.3	9
110	Ultrasound Video Summarization Using Deep Reinforcement Learning. Lecture Notes in Computer Science, 2020, , 483-492.	1.3	17
111	Deep Generative Model-Based Quality Control for Cardiac MRI Segmentation. Lecture Notes in Computer Science, 2020, , 88-97.	1.3	9
112	Image-Level Harmonization of Multi-site Data Using Image-and-Spatial Transformer Networks. Lecture Notes in Computer Science, 2020, , 710-719.	1.3	9
113	Unsupervised Cross-domain Image Classification by Distance Metric Guided Feature Alignment. Lecture Notes in Computer Science, 2020, , 146-157.	1.3	5
114	Automated Detection of Congenital Heart Disease in Fetal Ultrasound Screening. Lecture Notes in Computer Science, 2020, , 243-252.	1.3	5
115	Patch-Based Brain Age Estimation fromÂMRÂlmages. Lecture Notes in Computer Science, 2020, , 98-107.	1.3	11
116	Communicative Reinforcement Learning Agents for Landmark Detection in Brain Images. Lecture Notes in Computer Science, 2020, , 177-186.	1.3	8
117	Informed consent procedures in patients with an acute inability to provide informed consent: Policy and practice in the CENTER-TBI study. Journal of Critical Care, 2020, 59, 6-15.	2.2	8
118	A Systematic Comparison of Encrypted Machine Learning Solutions for Image Classification. , 2020, , .		12
119	Cortical morphology at birth reflects spatiotemporal patterns of gene expression in the fetal human brain. PLoS Biology, 2020, 18, e3000976.	5.6	38
120	Interpretable Deep Models for Cardiac Resynchronisation Therapy Response Prediction. Lecture Notes in Computer Science, 2020, 2020, 284-293.	1.3	14
121	Transfer Learning for Brain Segmentation: Pre-task Selection and Data Limitations. Communications in Computer and Information Science, 2020, , 118-130.	0.5	3
122	Spatial Semantic-Preserving Latent Space Learning for Accelerated DWI Diagnostic Report Generation. Lecture Notes in Computer Science, 2020, , 333-342.	1.3	2
123	Assessing the Impact of Blood Pressure on Cardiac Function Using Interpretable Biomarkers and Variational Autoencoders. Lecture Notes in Computer Science, 2020, , 22-30.	1.3	1
124	Geometric Deep Learning for Post-Menstrual Age Prediction Based on the Neonatal White Matter Cortical Surface. Lecture Notes in Computer Science, 2020, , 174-186.	1.3	5
125	Convolutional Recurrent Neural Networks for Dynamic MR Image Reconstruction. IEEE Transactions on Medical Imaging, 2019, 38, 280-290.	8.9	362
126	Automated processing pipeline for neonatal diffusion MRI in the developing Human Connectome Project. Neurolmage, 2019, 185, 750-763.	4.2	127

#	Article	IF	CITATIONS
127	Ageâ€related craniofacial differences based on spatioâ€temporal face image atlases. IET Image Processing, 2019, 13, 1561-1568.	2.5	0
128	Sex and regional differences in myocardial plasticity in aortic stenosis are revealed by 3D model machine learning. European Heart Journal Cardiovascular Imaging, 2019, 21, 417-427.	1.2	7
129	Unsupervised Deformable Registration for Multi-modal Images via Disentangled Representations. Lecture Notes in Computer Science, 2019, , 249-261.	1.3	59
130	Self-supervised learning for medical image analysis using image context restoration. Medical Image Analysis, 2019, 58, 101539.	11.6	315
131	Machine learning in cardiovascular magnetic resonance: basic concepts and applications. Journal of Cardiovascular Magnetic Resonance, 2019, 21, 61.	3.3	157
132	Scar shape analysis and simulated electrical instabilities in a non-ischemic dilated cardiomyopathy patient cohort. PLoS Computational Biology, 2019, 15, e1007421.	3.2	10
133	3D High-Resolution Cardiac Segmentation Reconstruction From 2D Views Using Conditional Variational Autoencoders. , 2019, , .		11
134	Case-mix, care pathways, and outcomes in patients with traumatic brain injury in CENTER-TBI: a European prospective, multicentre, longitudinal, cohort study. Lancet Neurology, The, 2019, 18, 923-934.	10.2	304
135	Brain Connectivity Measures Improve Modeling of Functional Outcome After Acute Ischemic Stroke. Stroke, 2019, 50, 2761-2767.	2.0	24
136	A Multicenter, Scan-Rescan, Human and Machine Learning CMR Study to Test Generalizability and Precision in Imaging Biomarker Analysis. Circulation: Cardiovascular Imaging, 2019, 12, e009214.	2.6	75
137	Automatic 3D Bi-Ventricular Segmentation of Cardiac Images by a Shape-Refined Multi- Task Deep Learning Approach. IEEE Transactions on Medical Imaging, 2019, 38, 2151-2164.	8.9	155
138	Attention gated networks: Learning to leverage salient regions in medical images. Medical Image Analysis, 2019, 53, 197-207.	11.6	1,011
139	Computational anatomy for multi-organ analysis in medical imaging: A review. Medical Image Analysis, 2019, 56, 44-67.	11.6	48
140	Automatic CNN-based detection of cardiac MR motion artefacts using k-space data augmentation and curriculum learning. Medical Image Analysis, 2019, 55, 136-147.	11.6	71
141	Weakly Supervised Estimation of Shadow Confidence Maps in Fetal Ultrasound Imaging. IEEE Transactions on Medical Imaging, 2019, 38, 2755-2767.	8.9	38
142	Impact of a clinical decision support tool on prediction of progression in early-stage dementia: a prospective validation study. Alzheimer's Research and Therapy, 2019, 11, 25.	6.2	23
143	Automated quality control in image segmentation: application to the UK Biobank cardiovascular magnetic resonance imaging study. Journal of Cardiovascular Magnetic Resonance, 2019, 21, 18.	3.3	78
144	Cardiac Rhythm Device Identification Using Neural Networks. JACC: Clinical Electrophysiology, 2019, 5, 576-586.	3.2	36

#	Article	IF	CITATIONS
145	Ventricular remodeling in preterm infants: computational cardiac magnetic resonance atlasing shows significant early remodeling of the left ventricle. Pediatric Research, 2019, 85, 807-815.	2.3	41
146	Evaluating reinforcement learning agents for anatomical landmark detection. Medical Image Analysis, 2019, 53, 156-164.	11.6	121
147	Impact of a Clinical Decision Support Tool on Dementia Diagnostics in Memory Clinics: The PredictND Validation Study. Current Alzheimer Research, 2019, 16, 91-101.	1.4	23
148	Deep-learning cardiac motion analysis for human survival prediction. Nature Machine Intelligence, 2019, 1, 95-104.	16.0	179
149	Independent Left Ventricular Morphometric Atlases Show Consistent Relationships with Cardiovascular Risk Factors: A UK Biobank Study. Scientific Reports, 2019, 9, 1130.	3.3	43
150	Metabolic pathways associated with right ventricular adaptation to pulmonary hypertension: 3D analysis of cardiac magnetic resonance imaging. European Heart Journal Cardiovascular Imaging, 2019, 20, 668-676.	1.2	13
151	Learning-Based Quality Control for Cardiac MR Images. IEEE Transactions on Medical Imaging, 2019, 38, 1127-1138.	8.9	42
152	Central versus Local Radiological Reading of Acute Computed Tomography Characteristics in Multi-Center Traumatic Brain Injury Research. Journal of Neurotrauma, 2019, 36, 1080-1092.	3.4	30
153	k-t NEXT: Dynamic MR Image Reconstruction Exploiting Spatio-Temporal Correlations. Lecture Notes in Computer Science, 2019, , 505-513.	1.3	18
154	Learning Shape Priors for Robust Cardiac MR Segmentation from Multi-view Images. Lecture Notes in Computer Science, 2019, , 523-531.	1.3	28
155	Self-Supervised Learning for Cardiac MR Image Segmentation by Anatomical Position Prediction. Lecture Notes in Computer Science, 2019, , 541-549.	1.3	78
156	Data Efficient Unsupervised Domain Adaptation For Cross-modality Image Segmentation. Lecture Notes in Computer Science, 2019, , 669-677.	1.3	59
157	Multiple Landmark Detection Using Multi-agent Reinforcement Learning. Lecture Notes in Computer Science, 2019, , 262-270.	1.3	34
158	Detection and Correction of Cardiac MRI Motion Artefacts During Reconstruction from k-space. Lecture Notes in Computer Science, 2019, , 695-703.	1.3	16
159	Exploiting Motion for Deep Learning Reconstruction of Extremely-Undersampled Dynamic MRI. Lecture Notes in Computer Science, 2019, , 704-712.	1.3	15
160	VS-Net: Variable Splitting Network for Accelerated Parallel MRI Reconstruction. Lecture Notes in Computer Science, 2019, , 713-722.	1.3	42
161	Intelligent Image Synthesis to Attack a Segmentation CNN Using Adversarial Learning. Lecture Notes in Computer Science, 2019, , 90-99.	1.3	12
162	Representation Disentanglement for Multi-task Learning with Application to Fetal Ultrasound. Lecture Notes in Computer Science, 2019, , 47-55.	1.3	3

#	Article	IF	CITATIONS
163	Flexible Conditional Image Generation of Missing Data with Learned Mental Maps. Lecture Notes in Computer Science, 2019, , 139-150.	1.3	Ο
164	Dynamic patterns of cortical expansion during folding of the preterm human brain. Proceedings of the National Academy of Sciences of the United States of America, 2018, 115, 3156-3161.	7.1	94
165	Automatic MRI Quantifying Methods in Behavioral-Variant Frontotemporal Dementia Diagnosis. Dementia and Geriatric Cognitive Disorders Extra, 2018, 8, 51-59.	1.3	19
166	The developing human connectome project: A minimal processing pipeline for neonatal cortical surface reconstruction. Neurolmage, 2018, 173, 88-112.	4.2	315
167	A Deep Cascade of Convolutional Neural Networks for Dynamic MR Image Reconstruction. IEEE Transactions on Medical Imaging, 2018, 37, 491-503.	8.9	816
168	Multi-Atlas Segmentation Using Partially Annotated Data: Methods and Annotation Strategies. IEEE Transactions on Pattern Analysis and Machine Intelligence, 2018, 40, 1683-1696.	13.9	8
169	Anatomically Constrained Neural Networks (ACNNs): Application to Cardiac Image Enhancement and Segmentation. IEEE Transactions on Medical Imaging, 2018, 37, 384-395.	8.9	493
170	A large margin algorithm for automated segmentation of white matter hyperintensity. Pattern Recognition, 2018, 77, 150-159.	8.1	19
171	Metric learning with spectral graph convolutions on brain connectivity networks. NeuroImage, 2018, 169, 431-442.	4.2	237
172	3-D Reconstruction in Canonical Co-Ordinate Space From Arbitrarily Oriented 2-D Images. IEEE Transactions on Medical Imaging, 2018, 37, 1737-1750.	8.9	60
173	Human brain mapping: A systematic comparison of parcellation methods for the human cerebral cortex. NeuroImage, 2018, 170, 5-30.	4.2	280
174	Statistical Shape Modeling of the Left Ventricle: Myocardial Infarct Classification Challenge. IEEE Journal of Biomedical and Health Informatics, 2018, 22, 503-515.	6.3	61
175	Distortion Correction in Fetal EPI Using Non-Rigid Registration With a Laplacian Constraint. IEEE Transactions on Medical Imaging, 2018, 37, 12-19.	8.9	20
176	A review on automatic fetal and neonatal brain MRI segmentation. Neurolmage, 2018, 170, 231-248.	4.2	143
177	Myocardial strain computed at multiple spatial scales from tagged magnetic resonance imaging: Estimating cardiac biomarkers for CRT patients. Medical Image Analysis, 2018, 43, 169-185.	11.6	7
178	Three-dimensional cardiovascular imaging-genetics: a mass univariate framework. Bioinformatics, 2018, 34, 97-103.	4.1	34
179	Multimodal surface matching with higher-order smoothness constraints. NeuroImage, 2018, 167, 453-465.	4.2	219
	Human-level Performance On Automatic Head Biometrics In Fetal Ultrasound Using Fully		

180 Human-level Performance On Automatic Head Biometrics In Fetal Ultrasound Using Fully Convolutional Neural Networks., 2018, 2018, 714-717.

37

#	Article	IF	CITATIONS
181	Combining Deep Learning and Shape Priors for Bi-Ventricular Segmentation of Volumetric Cardiac Magnetic Resonance Images. Lecture Notes in Computer Science, 2018, , 258-267.	1.3	3
182	Fibrosis Microstructure Modulates Reentry in Non-ischemic Dilated Cardiomyopathy: Insights From Imaged Guided 2D Computational Modeling. Frontiers in Physiology, 2018, 9, 1832.	2.8	25
183	Deep Learning Using K-Space Based Data Augmentation for Automated Cardiac MR Motion Artefact Detection. Lecture Notes in Computer Science, 2018, , 250-258.	1.3	13
184	Real-Time Prediction of Segmentation Quality. Lecture Notes in Computer Science, 2018, , 578-585.	1.3	23
185	A Comprehensive Approach for Learning-Based Fully-Automated Inter-slice Motion Correction for Short-Axis Cine Cardiac MR Image Stacks. Lecture Notes in Computer Science, 2018, , 268-276.	1.3	5
186	Small Organ Segmentation in Whole-Body MRI Using a Two-Stage FCN and Weighting Schemes. Lecture Notes in Computer Science, 2018, , 346-354.	1.3	16
187	Automatic Shadow Detection in 2D Ultrasound Images. Lecture Notes in Computer Science, 2018, , 66-75.	1.3	6
188	Standard Plane Detection in 3D Fetal Ultrasound Using an Iterative Transformation Network. Lecture Notes in Computer Science, 2018, , 392-400.	1.3	30
189	Learning Interpretable Anatomical Features Through Deep Generative Models: Application to Cardiac Remodeling. Lecture Notes in Computer Science, 2018, , 464-471.	1.3	35
190	3D Fetal Skull Reconstruction from 2DUS via Deep Conditional Generative Networks. Lecture Notes in Computer Science, 2018, , 383-391.	1.3	18
191	Automated cardiovascular magnetic resonance image analysis with fully convolutional networks. Journal of Cardiovascular Magnetic Resonance, 2018, 20, 65.	3.3	468
192	Joint Motion Estimation and Segmentation from Undersampled Cardiac MR Image. Lecture Notes in Computer Science, 2018, , 55-63.	1.3	14
193	Bayesian Deep Learning for Accelerated MR Image Reconstruction. Lecture Notes in Computer Science, 2018, , 64-71.	1.3	22
194	Cardiac MR Motion Artefact Correction from K-space Using Deep Learning-Based Reconstruction. Lecture Notes in Computer Science, 2018, , 21-29.	1.3	18
195	LSTM Spatial Co-transformer Networks for Registration of 3D Fetal US and MR Brain Images. Lecture Notes in Computer Science, 2018, , 149-159.	1.3	13
196	Cardiac MR Segmentation from Undersampled k-space Using Deep Latent Representation Learning. Lecture Notes in Computer Science, 2018, , 259-267.	1.3	15
197	Joint Learning of Motion Estimation and Segmentation for Cardiac MR Image Sequences. Lecture Notes in Computer Science, 2018, , 472-480.	1.3	74
198	Rapid Automated Quantification of Cerebral Leukoaraiosis on CT Images: A Multicenter Validation Study. Radiology, 2018, 288, 573-581.	7.3	25

#	Article	IF	CITATIONS
199	Disease prediction using graph convolutional networks: Application to Autism Spectrum Disorder and Alzheimer's disease. Medical Image Analysis, 2018, 48, 117-130.	11.6	391
200	Structural brain imaging in Alzheimer's disease and mild cognitive impairment: biomarker analysis and shared morphometry database. Scientific Reports, 2018, 8, 11258.	3.3	106
201	Data-Driven Differential Diagnosis of Dementia Using Multiclass Disease State Index Classifier. Frontiers in Aging Neuroscience, 2018, 10, 111.	3.4	29
202	DRINet for Medical Image Segmentation. IEEE Transactions on Medical Imaging, 2018, 37, 2453-2462.	8.9	198
203	Multi-modal Learning from Unpaired Images: Application to Multi-organ Segmentation in CT and MRI. , 2018, , .		61
204	Evaluating combinations of diagnostic tests to discriminate different dementia types. Alzheimer's and Dementia: Diagnosis, Assessment and Disease Monitoring, 2018, 10, 509-518.	2.4	19
205	Deep learning with ultrasound physics for fetal skull segmentation. , 2018, , .		20
206	Construction of a neonatal cortical surface atlas using Multimodal Surface Matching in the Developing Human Connectome Project. NeuroImage, 2018, 179, 11-29.	4.2	83
207	Graph Saliency Maps Through Spectral Convolutional Networks: Application toÂSex Classification with Brain Connectivity. Lecture Notes in Computer Science, 2018, , 3-13.	1.3	33
208	Adversarial and Perceptual Refinement for Compressed Sensing MRI Reconstruction. Lecture Notes in Computer Science, 2018, , 232-240.	1.3	50
209	Automatic View Planning with Multi-scale Deep Reinforcement Learning Agents. Lecture Notes in Computer Science, 2018, , 277-285.	1.3	27
210	Stochastic Deep Compressive Sensing for the Reconstruction of Diffusion Tensor Cardiac MRI. Lecture Notes in Computer Science, 2018, , 295-303.	1.3	22
211	Fast Multiple Landmark Localisation Using a Patch-Based Iterative Network. Lecture Notes in Computer Science, 2018, 2018, 563-571.	1.3	34
212	Computing CNN Loss and Gradients for Pose Estimation with Riemannian Geometry. Lecture Notes in Computer Science, 2018, , 756-764.	1.3	12
213	Recurrent Neural Networks for Aortic Image Sequence Segmentation with Sparse Annotations. Lecture Notes in Computer Science, 2018, , 586-594.	1.3	69
214	Deep Nested Level Sets: Fully Automated Segmentation of Cardiac MR Images in Patients with Pulmonary Hypertension. Lecture Notes in Computer Science, 2018, , 595-603.	1.3	17
215	Modelling the progression of Alzheimer's disease in MRI using generative adversarial networks. , 2018, , .		23
216	15â€Automatic mis-triggering artefact detection for image quality assessment of cardiac MRI. , 2018, , .		0

#	Article	IF	CITATIONS
217	A Novel Grading Biomarker for the Prediction of Conversion From Mild Cognitive Impairment to Alzheimer's Disease. IEEE Transactions on Biomedical Engineering, 2017, 64, 155-165.	4.2	120
218	A framework for combining a motion atlas with non-motion information to learn clinically useful biomarkers: Application to cardiac resynchronisation therapy response prediction. Medical Image Analysis, 2017, 35, 669-684.	11.6	35
219	Machine Learning of Three-dimensional Right Ventricular Motion Enables Outcome Prediction in Pulmonary Hypertension: A Cardiac MR Imaging Study. Radiology, 2017, 283, 381-390.	7.3	161
220	Reverse Classification Accuracy: Predicting Segmentation Performance in the Absence of Ground Truth. IEEE Transactions on Medical Imaging, 2017, 36, 1597-1606.	8.9	85
221	Five-class differential diagnostics of neurodegenerative diseases using random undersampling boosting. Neurolmage: Clinical, 2017, 15, 613-624.	2.7	38
222	Multi-atlas pancreas segmentation: Atlas selection based on vessel structure. Medical Image Analysis, 2017, 39, 18-28.	11.6	70
223	Spectral Graph Convolutions for Population-Based Disease Prediction. Lecture Notes in Computer Science, 2017, , 177-185.	1.3	104
224	Brain lesion segmentation through image synthesis and outlier detection. NeuroImage: Clinical, 2017, 16, 643-658.	2.7	38
225	Semi-supervised Learning for Network-Based Cardiac MR Image Segmentation. Lecture Notes in Computer Science, 2017, , 253-260.	1.3	209
226	Automatic Quality Control of Cardiac MRI Segmentation in Large-Scale Population Imaging. Lecture Notes in Computer Science, 2017, , 720-727.	1.3	12
227	A flexible graphical model for multi-modal parcellation of the cortex. NeuroImage, 2017, 162, 226-248.	4.2	7
228	SonoNet: Real-Time Detection and Localisation of Fetal Standard Scan Planes in Freehand Ultrasound. IEEE Transactions on Medical Imaging, 2017, 36, 2204-2215.	8.9	246
229	Fully automatic acute ischemic lesion segmentation in DWI using convolutional neural networks. NeuroImage: Clinical, 2017, 15, 633-643.	2.7	221
230	Fully automatic, multiorgan segmentation in normal whole body magnetic resonance imaging (<scp>MRI</scp>), using classification forests (<scp>CF</scp> s), convolutional neural networks (<scp>CNN</scp> s), and a multiâ€atlas (<scp>MA</scp>) approach. Medical Physics, 2017, 44, 5210-5220.	3.0	31
231	Learning and combining image neighborhoods using random forests for neonatal brain disease classification. Medical Image Analysis, 2017, 42, 189-199.	11.6	9
232	Impaired development of the cerebral cortex in infants with congenital heart disease is correlated to reduced cerebral oxygen delivery. Scientific Reports, 2017, 7, 15088.	3.3	60
233	A deformable model for the reconstruction of the neonatal cortex. , 2017, , .		29

234 Exploring heritability of functional brain networks with inexact graph matching. , 2017, , .

5

#	Article	IF	CITATIONS
235	Efficient multi-scale 3D CNN with fully connected CRF for accurate brain lesion segmentation. Medical Image Analysis, 2017, 36, 61-78.	11.6	2,382
236	DeepCut: Object Segmentation From Bounding Box Annotations Using Convolutional Neural Networks. IEEE Transactions on Medical Imaging, 2017, 36, 674-683.	8.9	260
237	Autoadaptive motion modelling for MR-based respiratory motion estimation. Medical Image Analysis, 2017, 35, 83-100.	11.6	25
238	Multi-modal classification of Alzheimer's disease using nonlinear graph fusion. Pattern Recognition, 2017, 63, 171-181.	8.1	166
239	Supervoxel classification forests for estimating pairwise image correspondences. Pattern Recognition, 2017, 63, 561-569.	8.1	21
240	ISLES 2015 - A public evaluation benchmark for ischemic stroke lesion segmentation from multispectral MRI. Medical Image Analysis, 2017, 35, 250-269.	11.6	360
241	Titin-truncating variants affect heart function in disease cohorts and the general population. Nature Genetics, 2017, 49, 46-53.	21.4	255
242	Stratified Decision Forests for Accurate Anatomical Landmark Localization in Cardiac Images. IEEE Transactions on Medical Imaging, 2017, 36, 332-342.	8.9	56
243	PVR: Patch-to-Volume Reconstruction for Large Area Motion Correction of Fetal MRI. IEEE Transactions on Medical Imaging, 2017, 36, 2031-2044.	8.9	33
244	Reproducible Large-Scale Neuroimaging Studies with the OpenMOLE Workflow Management System. Frontiers in Neuroinformatics, 2017, 11, 21.	2.5	5
245	Automated Detection of Motion Artefacts in MR Imaging Using Decision Forests. Journal of Medical Engineering, 2017, 2017, 1-9.	1.1	38
246	Regional brain morphometry in patients with traumatic brain injury based on acute- and chronic-phase magnetic resonance imaging. PLoS ONE, 2017, 12, e0188152.	2.5	25
247	Fully Convolutional Networks in Medical Imaging: Applications to Image Enhancement and Recognition. Advances in Computer Vision and Pattern Recognition, 2017, , 159-179.	1.3	5
248	Unsupervised Domain Adaptation in Brain Lesion Segmentation with Adversarial Networks. Lecture Notes in Computer Science, 2017, , 597-609.	1.3	241
249	A Deep Cascade of Convolutional Neural Networks for MR Image Reconstruction. Lecture Notes in Computer Science, 2017, , 647-658.	1.3	187
250	Learning-Based Heart Coverage Estimation for Short-Axis Cine Cardiac MR Images. Lecture Notes in Computer Science, 2017, , 73-82.	1.3	3
251	Predicting Slice-to-Volume Transformation inÂPresence of Arbitrary Subject Motion. Lecture Notes in Computer Science, 2017, , 296-304.	1.3	31
252	Fully Automated Segmentation-Based Respiratory Motion Correction of Multiplanar Cardiac Magnetic Resonance Images for Large-Scale Datasets. Lecture Notes in Computer Science, 2017, , 332-340.	1.3	16

#	Article	IF	CITATIONS
253	Joint Supervoxel Classification Forest for Weakly-Supervised Organ Segmentation. Lecture Notes in Computer Science, 2017, , 79-87.	1.3	4
254	3D FCN Feature Driven Regression Forest-Based Pancreas Localization and Segmentation. Lecture Notes in Computer Science, 2017, , 222-230.	1.3	4
255	Multi-channel MRI segmentation of eye structures and tumors using patient-specific features. PLoS ONE, 2017, 12, e0173900.	2.5	13
256	Learning Optimal Spatial Scales for Cardiac Strain Analysis Using a Motion Atlas. Lecture Notes in Computer Science, 2017, , 57-65.	1.3	0
257	Regional Differences in End-Diastolic Volumes between 3D Echo and CMR in HLHS Patients. Frontiers in Pediatrics, 2016, 4, 133.	1.9	6
258	Fast Fully Automatic Segmentation of the Severely Abnormal Human Right Ventricle from Cardiovascular Magnetic Resonance Images Using a Multi-Scale 3D Convolutional Neural Network. , 2016, , .		4
259	Discrete Optimisation for Group-Wise Cortical Surface Atlasing. , 2016, , .		2
260	Fast Deformable Image Registration with Non-smooth Dual Optimization. , 2016, , .		0
261	Real-Time Single Image and Video Super-Resolution Using an Efficient Sub-Pixel Convolutional Neural Network. , 2016, , .		3,557
262	Differential diagnosis of neurodegenerative diseases using structural MRI data. NeuroImage: Clinical, 2016, 11, 435-449.	2.7	137
263	Group-wise parcellation of the cortex through multi-scale spectral clustering. NeuroImage, 2016, 136, 68-83.	4.2	38
264	Construction of a neonatal cortical surface atlas using multimodal surface matching. , 2016, , .		5
265	A Multi-resolution Multi-model Method for Coronary Centerline Extraction Based on Minimal Path. Lecture Notes in Computer Science, 2016, , 320-328.	1.3	2
266	Relationship between body composition and left ventricular geometry using three dimensional cardiovascular magnetic resonance. Journal of Cardiovascular Magnetic Resonance, 2016, 18, 32.	3.3	23
267	Pseudo-healthy Image Synthesis for White Matter Lesion Segmentation. Lecture Notes in Computer Science, 2016, , 87-96.	1.3	19
268	Multi-input Cardiac Image Super-Resolution Using Convolutional Neural Networks. Lecture Notes in Computer Science, 2016, , 246-254.	1.3	119
269	A Weighted Mirror Descent Algorithm for Nonsmooth Convex Optimization Problem. Journal of Optimization Theory and Applications, 2016, 170, 900-915.	1.5	4
270	Evaluation of Six Registration Methods for the Human Abdomen on Clinically Acquired CT. IEEE Transactions on Biomedical Engineering, 2016, 63, 1563-1572.	4.2	111

#	Article	IF	CITATIONS
271	An exploration of task based fMRI in neonates using echo-shifting to allow acquisition at longer T E without loss of temporal efficiency. NeuroImage, 2016, 127, 298-306.	4.2	5
272	A robust similarity measure for volumetric image registration withÂoutliers. Image and Vision Computing, 2016, 52, 97-113.	4.5	7
273	Learning clinically useful information from images: Past, present and future. Medical Image Analysis, 2016, 33, 13-18.	11.6	22
274	Towards Left Ventricular Scar Localisation Using Local Motion Descriptors. Lecture Notes in Computer Science, 2016, , 30-39.	1.3	3
275	Regional growth and atlasing of the developing human brain. NeuroImage, 2016, 125, 456-478.	4.2	167
276	Dynamic Changes in White Matter Abnormalities Correlate With Late Improvement and Deterioration Following TBI. Neurorehabilitation and Neural Repair, 2016, 30, 49-62.	2.9	59
277	Standardized Evaluation System for Left Ventricular Segmentation Algorithms in 3D Echocardiography. IEEE Transactions on Medical Imaging, 2016, 35, 967-977.	8.9	82
278	Structure Specific Atlas Generation and Its Application to Pancreas Segmentation from Contrasted Abdominal CT Volumes. Lecture Notes in Computer Science, 2016, , 47-56.	1.3	5
279	Boundary Mapping Through Manifold Learning for Connectivity-Based Cortical Parcellation. Lecture Notes in Computer Science, 2016, , 115-122.	1.3	2
280	GraMPa: Graph-Based Multi-modal Parcellation of the Cortex Using Fusion Moves. Lecture Notes in Computer Science, 2016, , 148-156.	1.3	6
281	Regression Forest-Based Atlas Localization and Direction Specific Atlas Generation for Pancreas Segmentation. Lecture Notes in Computer Science, 2016, , 556-563.	1.3	20
282	Fast Fully Automatic Segmentation of the Human Placenta from Motion Corrupted MRI. Lecture Notes in Computer Science, 2016, , 589-597.	1.3	34
283	A Semi-supervised Large Margin Algorithm for White Matter Hyperintensity Segmentation. Lecture Notes in Computer Science, 2016, , 104-112.	1.3	2
284	DeepMedic for Brain Tumor Segmentation. Lecture Notes in Computer Science, 2016, , 138-149.	1.3	170
285	Learning Biomarker Models for Progression Estimation of Alzheimer's Disease. PLoS ONE, 2016, 11, e0153040.	2.5	21
286	Differential Dementia Diagnosis on Incomplete Data with Latent Trees. Lecture Notes in Computer Science, 2016, , 44-52.	1.3	1
287	Beyond the AHA 17-Segment Model: Motion-Driven Parcellation of the Left Ventricle. Lecture Notes in Computer Science, 2016, , 13-20.	1.3	2
288	Eidolon: Visualization and Computational Framework for Multi-modal Biomedical Data Analysis. Lecture Notes in Computer Science, 2016, , 425-437.	1.3	7

#	Article	IF	CITATIONS
289	A bi-ventricular cardiac atlas built from 1000+ high resolution MR images of healthy subjects and an analysis of shape and motion. Medical Image Analysis, 2015, 26, 133-145.	11.6	119
290	Precursors of Hypertensive Heart Phenotype Develop in Healthy Adults. JACC: Cardiovascular Imaging, 2015, 8, 1260-1269.	5.3	40
291	Development of the Corticospinal and Callosal Tracts from Extremely Premature Birth up to 2 Years of Age. PLoS ONE, 2015, 10, e0125681.	2.5	22
292	Brain Extraction Using Label Propagation and Group Agreement: Pincram. PLoS ONE, 2015, 10, e0129211.	2.5	43
293	Discriminative dictionary learning for abdominal multi-organ segmentation. Medical Image Analysis, 2015, 23, 92-104.	11.6	122
294	Geodesic Information Flows: Spatially-Variant Graphs and Their Application to Segmentation and Fusion. IEEE Transactions on Medical Imaging, 2015, 34, 1976-1988.	8.9	265
295	Manifold Learning for Cardiac Modeling and Estimation Framework. Lecture Notes in Computer Science, 2015, , 284-294.	1.3	3
296	4D Blood Flow Reconstruction Over the Entire Ventricle From Wall Motion and Blood Velocity Derived From Ultrasound Data. IEEE Transactions on Medical Imaging, 2015, 34, 2298-2308.	8.9	24
297	T2* relaxometry of fetal brain at 1.5 Tesla using a motion tolerant method. Magnetic Resonance in Medicine, 2015, 73, 1795-1802.	3.0	18
298	Robust whole-brain segmentation: Application to traumatic brain injury. Medical Image Analysis, 2015, 21, 40-58.	11.6	146
299	Multiatlas whole heart segmentation of CT data using conditional entropy for atlas ranking and selection. Medical Physics, 2015, 42, 3822-3833.	3.0	66
300	Joint Spectral Decomposition for the Parcellation of the Human Cerebral Cortex Using Resting-State fMRI. Lecture Notes in Computer Science, 2015, 24, 85-97.	1.3	27
301	Multi-atlas Segmentation as a Graph Labelling Problem: Application to Partially Annotated Atlas Data. Lecture Notes in Computer Science, 2015, 24, 221-232.	1.3	13
302	Self-Aligning Manifolds for Matching Disparate Medical Image Datasets. Lecture Notes in Computer Science, 2015, 24, 363-374.	1.3	11
303	Multi-stage Biomarker Models for Progression Estimation in Alzheimer's Disease. Lecture Notes in Computer Science, 2015, 24, 387-398.	1.3	13
304	Evaluating Imputation Techniques for Missing Data in ADNI: A Patient Classification Study. Lecture Notes in Computer Science, 2015, , 3-10.	1.3	17
305	Identification of Cerebral Small Vessel Disease Using Multiple Instance Learning. Lecture Notes in Computer Science, 2015, , 523-530.	1.3	12
306	Nonlinear Graph Fusion for Multi-modal Classification of Alzheimer's Disease. Lecture Notes in Computer Science, 2015, , 77-84.	1.3	14

#	Article	IF	CITATIONS
307	Supervoxel Classification Forests for Estimating Pairwise Image Correspondences. Lecture Notes in Computer Science, 2015, , 94-101.	1.3	6
308	Fast Volume Reconstruction From Motion Corrupted Stacks of 2D Slices. IEEE Transactions on Medical Imaging, 2015, 34, 1901-1913.	8.9	138
309	Right ventricle segmentation from cardiac MRI: A collation study. Medical Image Analysis, 2015, 19, 187-202.	11.6	189
310	Evaluation of automatic neonatal brain segmentation algorithms: The NeoBrainS12 challenge. Medical Image Analysis, 2015, 20, 135-151.	11.6	85
311	Multi-atlas segmentation with augmented features for cardiac MR images. Medical Image Analysis, 2015, 19, 98-109.	11.6	137
312	Tractography-Driven Groupwise Multi-scale Parcellation of the Cortex. Lecture Notes in Computer Science, 2015, 24, 600-612.	1.3	19
313	Flexible Reconstruction and Correction of Unpredictable Motion from Stacks ofÂ2D Images. Lecture Notes in Computer Science, 2015, , 555-562.	1.3	7
314	Prospective Identification of CRT Super Responders Using a Motion Atlas and Random Projection Ensemble Learning. Lecture Notes in Computer Science, 2015, , 493-500.	1.3	8
315	Multi-Level Parcellation of the Cerebral Cortex Using Resting-State fMRI. Lecture Notes in Computer Science, 2015, , 47-54.	1.3	9
316	Fast Reconstruction of Accelerated Dynamic MRI Using Manifold Kernel Regression. Lecture Notes in Computer Science, 2015, , 510-518.	1.3	6
317	Learning and Combining Image Similarities for Neonatal Brain Population Studies. Lecture Notes in Computer Science, 2015, , 110-117.	1.3	0
318	Prediction of Clinical Information from Cardiac MRI Using Manifold Learning. Lecture Notes in Computer Science, 2015, , 91-98.	1.3	3
319	Consistent and robust 4D whole-brain segmentation: Application to traumatic brain injury. , 2014, , .		3
320	Registration and Segmentation in Medical Imaging. Studies in Computational Intelligence, 2014, , 137-156.	0.9	7
321	Robustness of automated hippocampal volumetry across magnetic resonance field strengths and repeat images. Alzheimer's and Dementia, 2014, 10, 430.	0.8	33
322	Multi-atlas propagation via a manifold graph on a database of both labeled and unlabeled images. Proceedings of SPIE, 2014, , .	0.8	1
323	Multi-scale feature learning on pixels and super-pixels for seminal vesicles MRI segmentation. , 2014, , .		2

#	Article	IF	CITATIONS
325	Graph-Based Label Propagation in Fetal Brain MR Images. Lecture Notes in Computer Science, 2014, , 9-16.	1.3	6
326	Multiple instance learning for classification of dementia in brain MRI. Medical Image Analysis, 2014, 18, 808-818.	11.6	163
327	The relationship between lateral meniscus shape and joint contact parameters in the knee: a study using data from the Osteoarthritis Initiative. Arthritis Research and Therapy, 2014, 16, R27.	3.5	12
328	Population-based studies of myocardial hypertrophy: high resolution cardiovascular magnetic resonance atlases improve statistical power. Journal of Cardiovascular Magnetic Resonance, 2014, 16, 16.	3.3	42
329	Understanding the need of ventricular pressure for the estimation of diastolic biomarkers. Biomechanics and Modeling in Mechanobiology, 2014, 13, 747-757.	2.8	17
330	Automatic quantification of CT images for traumatic brain injury. , 2014, , .		2
331	Coronary centerline extraction based on ostium detection and model-guided directional minimal path. , 2014, , .		7
332	Hierarchical Manifold Learning for Regional Image Analysis. IEEE Transactions on Medical Imaging, 2014, 33, 444-461.	8.9	26
333	Patch-Based Evaluation of Image Segmentation. , 2014, , .		12
334	Dictionary Learning and Time Sparsity for Dynamic MR Data Reconstruction. IEEE Transactions on Medical Imaging, 2014, 33, 979-994.	8.9	173
335	Common Genetic Variants and Risk of Brain Injury After Preterm Birth. Pediatrics, 2014, 133, e1655-e1663.	2.1	43
336	Automated fetal brain segmentation from 2D MRI slices for motion correction. NeuroImage, 2014, 101, 633-643.	4.2	74
337	Automatic Whole Brain MRI Segmentation of the Developing Neonatal Brain. IEEE Transactions on Medical Imaging, 2014, 33, 1818-1831.	8.9	296
338	Super-resolution reconstruction of cardiac MRI using coupled dictionary learning. , 2014, , .		25
339	A prospective evaluation of cardiovascular magnetic resonance measures of dyssynchrony in the prediction of response to cardiac resynchronization therapy. Journal of Cardiovascular Magnetic Resonance, 2014, 16, 58.	3.3	41
340	Manifold population modeling as a neuro-imaging biomarker: Application to ADNI and ADNI-GO. NeuroImage, 2014, 94, 275-286.	4.2	41
341	Rich-club organization of the newborn human brain. Proceedings of the National Academy of Sciences of the United States of America, 2014, 111, 7456-7461.	7.1	300
342	Automatic quantification of normal cortical folding patterns from fetal brain MRI. NeuroImage, 2014, 91, 21-32.	4.2	118

#	Article	IF	CITATIONS
343	High-resolution dynamic MR imaging of the thorax for respiratory motion correction of PET using groupwise manifold alignment. Medical Image Analysis, 2014, 18, 939-952.	11.6	36
344	Prediction of stroke thrombolysis outcome using CT brain machine learning. NeuroImage: Clinical, 2014, 4, 635-640.	2.7	131
345	Application-Driven MRI: Joint Reconstruction and Segmentation from Undersampled MRI Data. Lecture Notes in Computer Science, 2014, 17, 106-113.	1.3	12
346	Multi-atlas Spectral PatchMatch: Application to Cardiac Image Segmentation. Lecture Notes in Computer Science, 2014, 17, 348-355.	1.3	7
347	Geodesic Patch-Based Segmentation. Lecture Notes in Computer Science, 2014, 17, 666-673.	1.3	29
348	Motion Corrected 3D Reconstruction of the Fetal Thorax from Prenatal MRI. Lecture Notes in Computer Science, 2014, 17, 284-291.	1.3	18
349	Manifold Alignment and Transfer Learning for Classification of Alzheimer's Disease. Lecture Notes in Computer Science, 2014, , 77-84.	1.3	18
350	Fast Catheter Tracking in Echocardiographic Sequences for Cardiac Catheterization Interventions. Lecture Notes in Computer Science, 2014, , 171-179.	1.3	0
351	A Probabilistic Patch-Based Label Fusion Model for Multi-Atlas Segmentation With Registration Refinement: Application to Cardiac MR Images. IEEE Transactions on Medical Imaging, 2013, 32, 1302-1315.	8.9	174
352	Multi-atlas based neointima segmentation in intravascular coronary OCT. , 2013, , .		1
353	Automated analysis of atrial late gadolinium enhancement imaging that correlates with endocardial voltage and clinical outcomes: A 2-center study. Heart Rhythm, 2013, 10, 1184-1191.	0.7	120
354	Evaluation of current algorithms for segmentation of scar tissue from late Gadolinium enhancement cardiovascular magnetic resonance of the left atrium: an open-access grand challenge. Journal of Cardiovascular Magnetic Resonance, 2013, 15, 105.	3.3	136
355	A Framework for Inter-Subject Prediction of Functional Connectivity From Structural Networks. IEEE Transactions on Medical Imaging, 2013, 32, 2200-2214.	8.9	29
356	Catheter tracking in 3D echocardiographic sequences based on tracking in 2D X-ray sequences for cardiac catheterization interventions. , 2013, , .		2
357	Automated Abdominal Multi-Organ Segmentation With Subject-Specific Atlas Generation. IEEE Transactions on Medical Imaging, 2013, 32, 1723-1730.	8.9	225
358	Modeling of the bony pelvis from MRI using a multi-atlas AE-SDM for registration and tracking in image-guided robotic prostatectomy. Computerized Medical Imaging and Graphics, 2013, 37, 183-194.	5.8	11
359	The influence of preterm birth on the developing thalamocortical connectome. Cortex, 2013, 49, 1711-1721.	2.4	202
360	Measurements of medial temporal lobe atrophy for prediction of Alzheimer's disease in subjects with mild cognitive impairment. Neurobiology of Aging, 2013, 34, 2003-2013.	3.1	86

#	Article	IF	CITATIONS
361	The estimation of patient-specific cardiac diastolic functions from clinical measurements. Medical Image Analysis, 2013, 17, 133-146.	11.6	91
362	Benchmarking framework for myocardial tracking and deformation algorithms: An open access database. Medical Image Analysis, 2013, 17, 632-648.	11.6	140
363	Segmentation of MR images via discriminative dictionary learning and sparse coding: Application to hippocampus labeling. NeuroImage, 2013, 76, 11-23.	4.2	196
364	Temporal sparse free-form deformations. Medical Image Analysis, 2013, 17, 779-789.	11.6	50
365	Random forest-based similarity measures for multi-modal classification of Alzheimer's disease. NeuroImage, 2013, 65, 167-175.	4.2	376
366	Data-specific feature point descriptor matching using dictionary learning and graphical models. , 2013, , ,		0
367	Cardiac Image Super-Resolution with Global Correspondence Using Multi-Atlas PatchMatch. Lecture Notes in Computer Science, 2013, 16, 9-16.	1.3	150
368	The PredictAD project: development of novel biomarkers and analysis software for early diagnosis of the Alzheimer's disease. Interface Focus, 2013, 3, 20120072.	3.0	26
369	Multi-organ segmentation from 3D abdominal CT images using patient-specific weighted-probabilistic atlas. Proceedings of SPIE, 2013, , .	0.8	9
370	Localisation of the Brain in Fetal MRI Using Bundled SIFT Features. Lecture Notes in Computer Science, 2013, 16, 582-589.	1.3	19
371	3D cardiac cine reconstruction from free-breathing 2D real-time image acquisitions using iterative motion correction. , 2013, , .		0
372	Computation on shape manifold for atlas generation: application to whole heart segmentation of cardiac MRI. , 2013, , .		1
373	Improving whole-brain segmentations through incorporating regional image intensity statistics. Proceedings of SPIE, 2013, , .	0.8	1
374	Landmark detection and coupled patch registration for cardiac motion tracking. Proceedings of SPIE, 2013, , .	0.8	3
375	Magnetic Resonance Imaging of the Newborn Brain: Automatic Segmentation of Brain Images into 50 Anatomical Regions. PLoS ONE, 2013, 8, e59990.	2.5	78
376	Patch-Based Segmentation without Registration: Application to Knee MRI. Lecture Notes in Computer Science, 2013, , 98-105.	1.3	12
377	Spatially Aware Patch-Based Segmentation (SAPS): An Alternative Patch-Based Segmentation Framework. Lecture Notes in Computer Science, 2013, , 93-103.	1.3	9
378	Groupwise Simultaneous Manifold Alignment for High-Resolution Dynamic MR Imaging of Respiratory Motion. Lecture Notes in Computer Science, 2013, 23, 232-243.	1.3	13

#	Article	IF	CITATIONS
379	Flow Analysis in Cardiac Chambers Combining Phase Contrast, 3D Tagged and Cine MRI. Lecture Notes in Computer Science, 2013, , 360-369.	1.3	2
380	Multi-organ Segmentation Based on Spatially-Divided Probabilistic Atlas from 3D Abdominal CT Images. Lecture Notes in Computer Science, 2013, 16, 165-172.	1.3	62
381	Multiple Instance Learning for Classification of Dementia in Brain MRI. Lecture Notes in Computer Science, 2013, 16, 599-606.	1.3	9
382	Model-Guided Directional Minimal Path for Fully Automatic Extraction of Coronary Centerlines from Cardiac CTA. Lecture Notes in Computer Science, 2013, 16, 542-549.	1.3	7
383	Multiple Sclerosis Lesion Segmentation Using Dictionary Learning and Sparse Coding. Lecture Notes in Computer Science, 2013, 16, 735-742.	1.3	42
384	Testing the Sensitivity of Tract-Based Spatial Statistics to Simulated Treatment Effects in Preterm Neonates. PLoS ONE, 2013, 8, e67706.	2.5	27
385	Normalisation of Neonatal Brain Network Measures Using Stochastic Approaches. Lecture Notes in Computer Science, 2013, 16, 574-581.	1.3	2
386	Real-Time Catheter Extraction from 2D X-Ray Fluoroscopic and 3D Echocardiographic Images for Cardiac Interventions. Lecture Notes in Computer Science, 2013, , 198-206.	1.3	3
387	Injury markers predict time to dementia in subjects with MCI and amyloid pathology. Neurology, 2012, 79, 1809-1816.	1.1	129
388	Landmark localisation in brain MR images using feature point descriptors based on 3D local self-similarities. , 2012, , .		4
389	Hippocampal atrophy rate using an expectation maximization classifier with a disease-specific prior. , 2012, , .		1
390	Multi-organ Abdominal CT Segmentation Using Hierarchically Weighted Subject-Specific Atlases. Lecture Notes in Computer Science, 2012, 15, 10-17.	1.3	50
391	The Effect of Preterm Birth on Thalamic and Cortical Development. Cerebral Cortex, 2012, 22, 1016-1024.	2.9	262
392	Robust Global Registration through Geodesic Paths on an Empirical Manifold with Knee MRI from the Osteoarthritis Initiative (OAI). Lecture Notes in Computer Science, 2012, , 1-10.	1.3	1
393	Nonrigid free-form registration using landmark-based statistical deformation models. Proceedings of SPIE, 2012, , .	0.8	4
394	Localised manifold learning for cardiac image analysis. , 2012, , .		2
395	Automatic detection of coronary stent struts in intravascular OCT imaging. , 2012, , .		4
396	Optimizing the Diagnosis of Early Alzheimer's Disease in Mild Cognitive Impairment Subjects. Journal of Alzheimer's Disease, 2012, 32, 969-979.	2.6	32

#	Article	IF	CITATIONS
397	A Comprehensive Cardiac Motion Estimation Framework Using Both Untagged and 3-D Tagged MR Images Based on Nonrigid Registration. IEEE Transactions on Medical Imaging, 2012, 31, 1263-1275.	8.9	74
398	Fast and accurate global geodesic registrations using knee MRI from the Osteoarthritis Initiative. , 2012, , .		4
399	Recognition of 3D facial expression dynamics. Image and Vision Computing, 2012, 30, 762-773.	4.5	91
400	Multi-class brain segmentation using atlas propagation and EM-based refinement. , 2012, , .		20
401	Automatic segmentation of pediatric brain MRIs using a maximum probability pediatric atlas. , 2012, , .		4
402	LISA: Longitudinal image registration via spatio-temporal atlases. , 2012, , .		11
403	Test sequence of CSF and MRI biomarkers for prediction of AD in subjects with MCI. Neurobiology of Aging, 2012, 33, 2272-2281.	3.1	75
404	A new automated system to identify a consistent sampling position to make tissue Doppler and transmitral Doppler measurements of E, E′ and E/E′. International Journal of Cardiology, 2012, 155, 394-399.	1.7	8
405	Remodeling after acute myocardial infarction: mapping ventricular dilatation using three dimensional CMR image registration. Journal of Cardiovascular Magnetic Resonance, 2012, 14, 46.	3.3	24
406	Construction of a consistent high-definition spatio-temporal atlas of the developing brain using adaptive kernel regression. NeuroImage, 2012, 59, 2255-2265.	4.2	259
407	Automated measurement of local white matter lesion volume. NeuroImage, 2012, 59, 3901-3908.	4.2	14
408	Sparse reduced-rank regression detects genetic associations with voxel-wise longitudinal phenotypes in Alzheimer's disease. NeuroImage, 2012, 60, 700-716.	4.2	121
409	Multi-region analysis of longitudinal FDG-PET for the classification of Alzheimer's disease. NeuroImage, 2012, 60, 221-229.	4.2	136
410	Magnetic resonance imaging of the newborn brain: Manual segmentation of labelled atlases in term-born and preterm infants. NeuroImage, 2012, 62, 1499-1509.	4.2	175
411	Hippocampal atrophy in Alzheimer's disease. Neurodegenerative Disease Management, 2012, 2, 197-209.	2.2	2
412	Software Tool for Improved Prediction of Alzheimer's Disease. Neurodegenerative Diseases, 2012, 10, 149-152.	1.4	14
413	Geodesic Information Flows. Lecture Notes in Computer Science, 2012, 15, 262-270.	1.3	27
414	Structural MRI in Frontotemporal Dementia: Comparisons between Hippocampal Volumetry,	2.5	49

Structural MRI in Frontotemporal Dementia: Comparisons between Hippocampal Volumetry, Tensor-Based Morphometry and Voxel-Based Morphometry. PLoS ONE, 2012, 7, e52531. 414

#	Article	IF	CITATIONS
415	Reconstruction of a 3D surface from video that is robust to missing data and outliers: Application to minimally invasive surgery using stereo and mono endoscopes. Medical Image Analysis, 2012, 16, 597-611.	11.6	44
416	Nonlinear dimensionality reduction combining MR imaging with non-imaging information. Medical Image Analysis, 2012, 16, 819-830.	11.6	50
417	Diffeomorphic 3D Image Registration via Geodesic Shooting Using an Efficient Adjoint Calculation. International Journal of Computer Vision, 2012, 97, 229-241.	15.6	146
418	A Multi-image Graph Cut Approach for Cardiac Image Segmentation and Uncertainty Estimation. Lecture Notes in Computer Science, 2012, , 178-187.	1.3	4
419	Hierarchical Manifold Learning. Lecture Notes in Computer Science, 2012, 15, 512-519.	1.3	11
420	Unsupervised Learning of Shape Complexity: Application to Brain Development. Lecture Notes in Computer Science, 2012, , 88-99.	1.3	6
421	Classification and Lateralization of Temporal Lobe Epilepsies with and without Hippocampal Atrophy Based on Whole-Brain Automatic MRI Segmentation. PLoS ONE, 2012, 7, e33096.	2.5	59
422	Manifold Learning for Medical Image Registration, Segmentation, and Classification. Advances in Bioinformatics and Biomedical Engineering Book Series, 2012, , 351-372.	0.4	30
423	Solving MRF Minimization by Mirror Descent. Lecture Notes in Computer Science, 2012, , 587-598.	1.3	6
424	Gradient Projection Learning for Parametric Nonrigid Registration. Lecture Notes in Computer Science, 2012, , 226-233.	1.3	0
425	Automatic Cardiac Motion Tracking Using Both Untagged and 3D Tagged MR Images. Lecture Notes in Computer Science, 2012, , 45-54.	1.3	0
426	Validation of a Novel Method for the Automatic Segmentation of Left Atrial Scar from Delayed-Enhancement Magnetic Resonance. Lecture Notes in Computer Science, 2012, , 254-262.	1.3	1
427	Relating Brain Functional Connectivity to Anatomical Connections: Model Selection. Lecture Notes in Computer Science, 2012, , 178-185.	1.3	4
428	Learning Correspondences in Knee MR Images from the Osteoarthritis Initiative. Lecture Notes in Computer Science, 2012, , 218-225.	1.3	0
429	Tracking developmental changes in subcortical structures of the preterm brain using multi-modal MRI. , 2011, , .		8
430	A dynamic approach to the recognition of 3D facial expressions and their temporal models. , 2011, , .		46
431	Fast and robust extraction of hippocampus from MR images for diagnostics of Alzheimer's disease. NeuroImage, 2011, 56, 185-196.	4.2	109
432	Automatic morphometry in Alzheimer's disease and mild cognitive impairment. NeuroImage, 2011, 56, 2024-2037.	4.2	120

#	Article	IF	CITATIONS
433	Multi-template tensor-based morphometry: Application to analysis of Alzheimer's disease. NeuroImage, 2011, 56, 1134-1144.	4.2	88
434	A dynamic 4D probabilistic atlas of the developing brain. NeuroImage, 2011, 54, 2750-2763.	4.2	247
435	Multi-Method Analysis of MRI Images in Early Diagnostics of Alzheimer's Disease. PLoS ONE, 2011, 6, e25446.	2.5	240
436	Simultaneous Multi-scale Registration Using Large Deformation Diffeomorphic Metric Mapping. IEEE Transactions on Medical Imaging, 2011, 30, 1746-1759.	8.9	75
437	A Combined Manifold Learning Analysis of Shape and Appearance to Characterize Neonatal Brain Development. IEEE Transactions on Medical Imaging, 2011, 30, 2072-2086.	8.9	43
438	Automatical vessel wall detection in intravascular coronary OCT. , 2011, , .		16
439	A repository of MR morphometry data in Alzheimer's disease and mild cognitive impairment. , 2011, , .		0
440	Inference of functional connectivity from direct and indirect structural brain connections. , 2011, , .		10
441	Automated quantification and analysis of facial asymmetry in children with arthritis in the temporomandibular joint. , 2011, , .		2
442	Exploiting hierarchy in structural brain networks. , 2011, , .		0
443	Towards dense motion estimation in light and electron microscopy. , 2011, , .		6
444	Manifold learning combining imaging with non-imaging information. , 2011, , .		6
445	Incorporating hard constraints into non-rigid registration via nonlinear programming. , 2011, , .		0
446	Motion tracking of left ventricle and coronaries in 4D CTA. , 2011, , .		0
447	Improved generation of probabilistic atlases for the expectation maximization classification. , 2011, , .		4
448	Construction of a 4D atlas of the developing brain using non-rigid registration. , 2011, , .		0
449	Regional analysis of FDG-PET for use in the classification of Alzheimer'S Disease. , 2011, , .		16
450	Automatic segmentation and identification of solitary pulmonary nodules on follow-up CT scans based on local intensity structure analysis and non-rigid image registration. Proceedings of SPIE, 2011,	0.8	2

#	Article	IF	CITATIONS
451	Dense Multi-frame Optic Flow for Non-rigid Objects Using Subspace Constraints. Lecture Notes in Computer Science, 2011, , 460-473.	1.3	15
452	Automatic Segmentation of Different Pathologies from Cardiac Cine MRI Using Registration and Multiple Component EM Estimation. Lecture Notes in Computer Science, 2011, , 163-170.	1.3	17
453	A Framework Combining Multi-sequence MRI for Fully Automated Quantitative Analysis of Cardiac Global And Regional Functions. Lecture Notes in Computer Science, 2011, , 367-374.	1.3	3
454	An Automatic Data Assimilation Framework for Patient-Specific Myocardial Mechanical Parameter Estimation. Lecture Notes in Computer Science, 2011, , 392-400.	1.3	14
455	Automatic Segmentation of Left Atrial Scar from Delayed-Enhancement Magnetic Resonance Imaging. Lecture Notes in Computer Science, 2011, , 63-70.	1.3	7
456	A Probabilistic Framework to Infer Brain Functional Connectivity from Anatomical Connections. Lecture Notes in Computer Science, 2011, 22, 296-307.	1.3	20
457	Laplacian Eigenmaps Manifold Learning for Landmark Localization in Brain MR Images. Lecture Notes in Computer Science, 2011, 14, 566-573.	1.3	6
458	Random Forest-Based Manifold Learning for Classification of Imaging Data in Dementia. Lecture Notes in Computer Science, 2011, , 159-166.	1.3	16
459	Image guidance for robotic minimally invasive coronary artery bypass. Computerized Medical Imaging and Graphics, 2010, 34, 61-68.	5.8	34
460	Measuring atrophy by simultaneous segmentation of serial MR images using 4-D graph-cuts. , 2010, , .		0
461	Inference of functional connectivity from structural brain connectivity. , 2010, , .		7
462	Coronary artery motion modeling from 3D cardiac CT sequences using template matching and graph search. , 2010, , .		4
463	Atlas selection strategy for automatic segmentation of pediatric brain MRIs into 83 ROIs. , 2010, , .		5
464	Construction of a dynamic 4D probabilistic atlas for the developing brain. , 2010, , .		1
465	Improving intersubject image registration using tissue-class information benefits robustness and accuracy of multi-atlas based anatomical segmentation. NeuroImage, 2010, 51, 221-227.	4.2	174
466	Measurement of hippocampal atrophy using 4D graph-cut segmentation: Application to ADNI. NeuroImage, 2010, 52, 109-118.	4.2	122
467	A common neonatal image phenotype predicts adverse neurodevelopmental outcome in children born preterm. Neurolmage, 2010, 52, 409-414.	4.2	147
468	An optimised tract-based spatial statistics protocol for neonates: Applications to prematurity and chronic lung disease. NeuroImage, 2010, 53, 94-102.	4.2	154

#	Article	IF	CITATIONS
469	Nonrigid Registration of Medical Images: Theory, Methods, and Applications [Applications Corner. IEEE Signal Processing Magazine, 2010, 27, 113-119.	5.6	49
470	LEAP: Learning embeddings for atlas propagation. NeuroImage, 2010, 49, 1316-1325.	4.2	216
471	Fast and robust multi-atlas segmentation of brain magnetic resonance images. Neurolmage, 2010, 49, 2352-2365.	4.2	357
472	Identifying population differences in whole-brain structural networks: A machine learning approach. NeuroImage, 2010, 50, 910-919.	4.2	86
473	Medical Image Registration. Biological and Medical Physics Series, 2010, , 131-154.	0.4	22
474	Automated quantification and analysis of mandibular asymmetry. , 2010, , .		2
475	Manifold Learning for Biomarker Discovery in MR Imaging. Lecture Notes in Computer Science, 2010, , 116-123.	1.3	16
476	Nonrigid Registration and Template Matching for Coronary Motion Modeling from 4D CTA. Lecture Notes in Computer Science, 2010, , 210-221.	1.3	4
477	A Computational White Matter Atlas for Aging with Surface-Based Representation of Fasciculi. Lecture Notes in Computer Science, 2010, , 83-90.	1.3	17
478	Simultaneous Reconstruction of 4-D Myocardial Motion from Both Tagged and Untagged MR Images Using Nonrigid Image Registration. Lecture Notes in Computer Science, 2010, , 98-107.	1.3	2
479	A Robust Mosaicing Method with Super-Resolution for Optical Medical Images. Lecture Notes in Computer Science, 2010, , 373-382.	1.3	8
480	Coronary Motion Estimation from CTA Using Probability Atlas and Diffeomorphic Registration. Lecture Notes in Computer Science, 2010, , 78-87.	1.3	4
481	Simultaneous Fine and Coarse Diffeomorphic Registration: Application to Atrophy Measurement in Alzheimer's Disease. Lecture Notes in Computer Science, 2010, 13, 610-617.	1.3	20
482	Large Deformation Diffeomorphic Registration Using Fine and Coarse Strategies. Lecture Notes in Computer Science, 2010, , 186-197.	1.3	2
483	Automatic extraction of the left atrial anatomy from MR for atrial fibrillation ablation. , 2009, , .		3
484	Robust segmentation of brain structures in MRI. , 2009, , .		3
485	Segmentation of subcortical structures and the hippocampus in brain MRI using graph-cuts and subject-specific a-priori information. , 2009, , .		7
486	4D motion modeling of the coronary arteries from CT images for robotic assisted minimally invasive surgery. Proceedings of SPIE, 2009, , .	0.8	3

#	Article	IF	CITATIONS
487	Automatic segmentation of brain MRIs and mapping neuroanatomy across the human lifespan. , 2009, , .		1
488	Photo-consistency registration of a 4D cardiac motion model to endoscopic video for image guidance of robotic coronary artery bypass. , 2009, , .		0
489	Longitudinal regional brain volume changes quantified in normal aging and Alzheimer's APP×PS1 mice using MRI. Brain Research, 2009, 1270, 19-32.	2.2	97
490	Diffusion tensor imaging (DTI) of the brain in moving subjects: Application to inâ€utero fetal and exâ€utero studies. Magnetic Resonance in Medicine, 2009, 62, 645-655.	3.0	88
491	Atlas-based registration parameters in segmenting sub-cortical regions from brain MRI-images. , 2009, ,		2
492	Reconfigurable acceleration of 3D image registration. , 2009, , .		0
493	Analysis of serial magnetic resonance images of mouse brains using image registration. NeuroImage, 2009, 44, 692-700.	4.2	26
494	Evaluation of 14 nonlinear deformation algorithms applied to human brain MRI registration. NeuroImage, 2009, 46, 786-802.	4.2	1,988
495	Multi-atlas based segmentation of brain images: Atlas selection and its effect on accuracy. NeuroImage, 2009, 46, 726-738.	4.2	797
496	An evaluation of four automatic methods of segmenting the subcortical structures in the brain. NeuroImage, 2009, 47, 1435-1447.	4.2	180
497	Non-rigid Reconstruction of the Beating Heart Surface for Minimally Invasive Cardiac Surgery. Lecture Notes in Computer Science, 2009, 12, 34-42.	1.3	15
498	Tensor-Based Morphometry of Fibrous Structures with Application to Human Brain White Matter. Lecture Notes in Computer Science, 2009, 12, 466-473.	1.3	2
499	Automatic volumetry on MR brain images can support diagnostic decision making. BMC Medical Imaging, 2008, 8, 9.	2.7	17
500	Hierarchical statistical shape analysis and prediction of sub-cortical brain structures. Medical Image Analysis, 2008, 12, 55-68.	11.6	54
501	Assessment of brain growth in early childhood using deformation-based morphometry. NeuroImage, 2008, 39, 348-358.	4.2	57
502	Automatic segmentation of brain MRIs of 2-year-olds into 83 regions of interest. Neurolmage, 2008, 40, 672-684.	4.2	301
503	Automated morphological analysis of magnetic resonance brain imaging using spectral analysis. NeuroImage, 2008, 43, 225-235.	4.2	30
504	Statistical shape modelling: How many modes should be retained?. , 2008, , .		2

29

#	Article	IF	CITATIONS
505	Augmented reality image guidance for minimally invasive coronary artery bypass. Proceedings of SPIE, 2008, , .	0.8	6
506	Deformation based morphmetry and atlas based label segmentation: Application to serial mouse brain images. , 2008, , .		0
507	Predicting the shapes of bones at a joint: application to the shoulder. Computer Methods in Biomechanics and Biomedical Engineering, 2008, 11, 19-30.	1.6	35
508	Construction of a patient-specific atlas of the brain: Application to normal aging. , 2008, , .		17
509	Coronary Motion Modelling for Augmented Reality Guidance of Endoscopic Coronary Artery Bypass. Lecture Notes in Computer Science, 2008, , 197-202.	1.3	2
510	Image Guidance for Robotic Minimally Invasive Coronary Artery Bypass. Lecture Notes in Computer Science, 2008, , 202-209.	1.3	4
511	Comparison and Evaluation of Segmentation Techniques for Subcortical Structures in Brain MRI. Lecture Notes in Computer Science, 2008, 11, 409-416.	1.3	40
512	Sample Sufficiency and Number of Modes to Retain in Statistical Shape Modelling. Lecture Notes in Computer Science, 2008, 11, 425-433.	1.3	4
513	Multivariate Statistical Analysis of Whole Brain Structural Networks Obtained Using Probabilistic Tractography. Lecture Notes in Computer Science, 2008, 11, 486-493.	1.3	12
514	Evaluation of Rigid and Non-rigid Motion Compensation of Cardiac Perfusion MRI. Lecture Notes in Computer Science, 2008, 11, 35-43.	1.3	17
515	A Novel Algorithm for Heart Motion Analysis Based on Geometric Constraints. Lecture Notes in Computer Science, 2008, 11, 720-728.	1.3	6
516	Spectral Clustering as a Diagnostic Tool in Cross-Sectional MR Studies: An Application to Mild Dementia. Lecture Notes in Computer Science, 2008, 11, 442-449.	1.3	1
517	Guest Editorial Special Issue on Mathematical Modeling in Biomedical Image Analysis. IEEE Transactions on Medical Imaging, 2007, 26, 1133-1135.	8.9	0
518	Segmentation of cardiac MR and CT image sequences using model-based registration of a 4D statistical model. , 2007, , .		11
519	Automated localization of periventricular and subcortical white matter lesions. , 2007, , .		2
520	Automatic detection and quantification of hippocampal atrophy on MRI in temporal lobe epilepsy: A proof-of-principle study. NeuroImage, 2007, 36, 38-47.	4.2	91
521	Automatic segmentation and reconstruction of the cortex from neonatal MRI. NeuroImage, 2007, 38, 461-477.	4.2	192
522	Groupwise Combined Segmentation and Registration for Atlas Construction. , 2007, 10, 532-540.		34

#	Article	IF	CITATIONS
523	Segmentation of Brain MRI in Young Children. Academic Radiology, 2007, 14, 1350-1366.	2.5	47
524	MRI of Moving Subjects Using Multislice Snapshot Images With Volume Reconstruction (SVR): Application to Fetal, Neonatal, and Adult Brain Studies. IEEE Transactions on Medical Imaging, 2007, 26, 967-980.	8.9	173
525	Early growth in brain volume is preserved in the majority of preterm infants. Annals of Neurology, 2007, 62, 185-192.	5.3	89
526	Acquisition and voxelwise analysis of multi-subject diffusion data with Tract-Based Spatial Statistics. Nature Protocols, 2007, 2, 499-503.	12.0	526
527	Multivariate Statistical Differences of MRI Samples of the Human Brain. Journal of Mathematical Imaging and Vision, 2007, 29, 95-106.	1.3	21
528	A multivariate statistical analysis of the developing human brain in preterm infants. Image and Vision Computing, 2007, 25, 981-994.	4.5	25
529	Automatic Cortical Segmentation in the Developing Brain. Lecture Notes in Computer Science, 2007, 20, 257-269.	1.3	16
530	Nonrigid Image Registration with Subdivision Lattices: Application to Cardiac MR Image Analysis. , 2007, 10, 335-342.		15
531	Classifier Selection Strategies for Label Fusion Using Large Atlas Databases. , 2007, 10, 523-531.		53
532	Similarity Metrics for Groupwise Non-rigid Registration. , 2007, 10, 544-552.		26
533	In-utero Three Dimension High Resolution Fetal Brain Diffusion Tensor Imaging. , 2007, 10, 18-26.		10
534	Extracting Discriminative Information from Medical Images: A Multivariate Linear Approach. , 2006, , .		3
535	Automatic Quantification of Changes in Bone in Serial MR Images of Joints. IEEE Transactions on Medical Imaging, 2006, 25, 1617-1626.	8.9	15
536	Tract-based spatial statistics: Voxelwise analysis of multi-subject diffusion data. NeuroImage, 2006, 31, 1487-1505.	4.2	5,755
537	Cerebral atrophy measurements using Jacobian integration: Comparison with the boundary shift integral. NeuroImage, 2006, 32, 159-169.	4.2	60
538	Abnormal deep grey matter development following preterm birth detected using deformation-based morphometry. Neurolmage, 2006, 32, 70-78.	4.2	220
539	Automatic anatomical brain MRI segmentation combining label propagation and decision fusion. NeuroImage, 2006, 33, 115-126.	4.2	794
540	3D Statistical Shape Modeling of Long Bones. Lecture Notes in Computer Science, 2006, , 306-314.	1.3	4

#	Article	IF	CITATIONS
541	Diffeomorphic Registration Using B-Splines. Lecture Notes in Computer Science, 2006, 9, 702-709.	1.3	190
542	Beyond theg-factor limit in sensitivity encoding using joint histogram entropy. Magnetic Resonance in Medicine, 2006, 55, 153-160.	3.0	14
543	Deformation Based Morphometry Analysis of Serial Magnetic Resonance Images of Mouse Brains. Lecture Notes in Computer Science, 2006, , 58-65.	1.3	3
544	Statistical Finite Element Model for Bone Shape and Biomechanical Properties. Lecture Notes in Computer Science, 2006, 9, 405-411.	1.3	14
545	Propagating labels of the human brain based on non-rigid MR image registration: an evaluation. , 2005, , .		1
546	Simulation of cardiac pathologies using an electromechanical biventricular model and XMR interventional imaging. Medical Image Analysis, 2005, 9, 467-480.	11.6	53
547	Spatio-temporal free-form registration of cardiac MR image sequences. Medical Image Analysis, 2005, 9, 441-456.	11.6	121
548	Construction of a 4D Statistical Atlas of the Cardiac Anatomy and Its Use in Classification. Lecture Notes in Computer Science, 2005, 8, 402-410.	1.3	56
549	A comparison of the tissue classification and the segmentation propagation techniques in MRI brain image segmentation. , 2005, , .		2
550	Fast generation of digitally reconstructed radiographs using attenuation fields with application to 2D-3D image registration. IEEE Transactions on Medical Imaging, 2005, 24, 1441-1454.	8.9	110
551	Generalised Overlap Measures for Assessment of Pairwise and Groupwise Image Registration and Segmentation. Lecture Notes in Computer Science, 2005, 8, 99-106.	1.3	26
552	Fast Spatio-temporal Free-Form Registration of Cardiac MR Image Sequences. Lecture Notes in Computer Science, 2005, , 414-424.	1.3	1
553	Detecting and Comparing the Onset of Myocardial Activation and Regional Motion Changes in Tagged MR for XMR-Guided RF Ablation. Lecture Notes in Computer Science, 2005, , 348-358.	1.3	2
554	3D/4D Cardiac Segmentation Using Active Appearance Models, Non-rigid Registration, and the Insight Toolkit. Lecture Notes in Computer Science, 2004, , 419-426.	1.3	10
555	Segmentation of 4D cardiac MR images using a probabilistic atlas and the EM algorithm. Medical Image Analysis, 2004, 8, 255-265.	11.6	249
556	Registration-Based Interpolation. IEEE Transactions on Medical Imaging, 2004, 23, 922-926.	8.9	87
557	Analysis of 3-D Myocardial Motion in Tagged MR Images Using Nonrigid Image Registration. IEEE Transactions on Medical Imaging, 2004, 23, 1245-1250.	8.9	135
558	Spatial Transformation of Motion and Deformation Fields Using Nonrigid Registration. IEEE Transactions on Medical Imaging, 2004, 23, 1065-1076.	8.9	50

#	Article	IF	CITATIONS
559	XMR guided cardiac electrophysiology study and radio frequency ablation. , 2004, 5369, 10.		10
560	Using a Maximum Uncertainty LDA-Based Approach to Classify and Analyse MR Brain Images. Lecture Notes in Computer Science, 2004, , 291-300.	1.3	17
561	Detecting regional changes in myocardial contraction patterns using MRI. , 2004, , .		5
562	Spatio-Temporal Free-Form Registration of Cardiac MR Image Sequences. Lecture Notes in Computer Science, 2004, , 911-919.	1.3	10
563	A Framework for Detailed Objective Comparison of Non-rigid Registration Algorithms in Neuroimaging. Lecture Notes in Computer Science, 2004, , 679-686.	1.3	25
564	Simulation of the Electromechanical Activity of the Heart Using XMR Interventional Imaging. Lecture Notes in Computer Science, 2004, , 786-794.	1.3	6
565	Automatic construction of 3-D statistical deformation models of the brain using nonrigid registration. IEEE Transactions on Medical Imaging, 2003, 22, 1014-1025.	8.9	350
566	Registration and tracking to integrate X-ray and MR images in an XMR facility. IEEE Transactions on Medical Imaging, 2003, 22, 1369-1378.	8.9	111
567	Fast calculation of digitally reconstructed radiographs using light fields. , 2003, , .		28
568	Spatio-temporal Alignment of 4D Cardiac MR Images. Lecture Notes in Computer Science, 2003, , 205-214.	1.3	13
569	Non-rigid Spatio-Temporal Alignment of 4D Cardiac MR Images. Lecture Notes in Computer Science, 2003, , 191-200.	1.3	6
570	Analysis of myocardial motion in tagged MR images using nonrigid image registration. , 2002, , .		30
571	Parameterizing reconfigurable designs for image warping. , 2002, , .		4
572	<title>Automated camera calibration for image-guided surgery using intensity-based registration</title> . , 2002, 4681, 463.		1
573	Three-dimensional cardiovascular image analysis. IEEE Transactions on Medical Imaging, 2002, 21, 1005-1010.	8.9	26
574	Automatic construction of multiple-object three-dimensional statistical shape models: application to cardiac modeling. IEEE Transactions on Medical Imaging, 2002, 21, 1151-1166.	8.9	325
575	Nonrigid Registration. Biomedical Engineering Series, 2001, , 281-301.	0.4	29
576	A Generic Framework for Non-rigid Registration Based on Non-uniform Multi-level Free-Form Deformations. Lecture Notes in Computer Science, 2001, , 573-581.	1.3	185

#	Article	IF	CITATIONS
577	Automatic 3D ASM Construction via Atlas-Based Landmarking and Volumetric Elastic Registration. Lecture Notes in Computer Science, 2001, , 78-91.	1.3	51
578	Comparison and Evaluation of Rigid, Affine, and Nonrigid Registration of Breast MR Images. Journal of Computer Assisted Tomography, 1999, 23, 800-805.	0.9	103
579	Motion and deformation tracking for short-axis echo-planar myocardial perfusion imaging. Medical Image Analysis, 1998, 2, 285-302.	11.6	31
580	<title>Multiscale approach to contour fitting for MR images</title> . , 1996, , .		6
581	Exploring a New Paradigm for the Fetal Anomaly Ultrasound Scan: Artificial Intelligence in Real Time. SSRN Electronic Journal, 0, , .	0.4	1
582	Respiratory Motion Correction for 2D Cine Cardiac MR Images using Probabilistic Edge Maps. , 0, , .		2